Metal-Organic Materials (MOMs) Enhance Proteolytic Selectivity, Efficiency, and Reusability of Trypsin: A Time-Resolved Study on Proteolysis

Qiaobin Li,[1] Zoe Armstrong,[1] Austin MacRae,[1] Angel Ugrinov,[1] Li Feng,[1] Bingcan Chen,[2] Ying Huang,[3] Hui Li,[2,*] Yanxiong Pan[4,*] Zhongyu Yang[1,*]

1. Department of Chemistry and Biochemistry, North Dakota State University, Fargo, ND, 58102, USA

2. Department of Plant Sciences, North Dakota State University, Fargo, ND, 58102, USA

3. Department of Civil, Construction, and Environmental Engineering, North Dakota State University, Fargo, ND, 58102, USA

4. State Key Laboratory of Polymer Physics and Chemistry, Changchun Institute of Applied Chemistry, Changchun, 130022, China

Corresponding to: zhongyu.yang@ndsu.edu; hui.li.3@ndsu.edu; yxpan@ciac.ac.cn

Key words: Metal-Organic Materials, proteolytic selectivity, proteolytic efficiency, SDSL-EPR, tandem MS

Abstract

Proteases are involved in essential biological functions in nature and have become drug targets recently. In spite of the promising progress, two challenges, (*i*) the intrinsic instability and (*ii*) the difficulty in monitoring the catalytic process in real time, still hinder the further understanding and engineering of protease functionalities. These challenges are caused by the lack of proper materials/approaches to stabilize proteases and monitor proteolytic products (truncated polypeptides) in real time in a highly heterogeneous reaction mixture. This work combines Metal-Organic Materials (MOMs), site-directed spin labeling (SDSL) - Electron Paramagnetic Resonance (EPR) spectroscopy, and Mass Spectrometry (MS) to overcome both barriers. A model protease, trypsin, which cleaves the peptide bonds at lysine or arginine residues, was immobilized on a Ca-MOM via aqueous-phase, one-pot co-crystallization, which allows for trypsin protection and ease of separation from its proteolytic products. Time-resolved EPR and MS were employed to monitor the populations, rotational motion, and sequences of the cleaved peptide truncations of a model protein substrate as the reaction proceeded. Our data suggest a significant (at least 5-10 times) enhancement in the catalytic efficiency (k_{cat}/k_m) of trypsin@Ca-MOM and excellent reusability as compared to free trypsin in solution. Surprisingly, entrapping trypsin in Ca-MOMs results in cleavage site/region selectivity against the protein substrate, as compared to the near non-selective cleavage of all lysine and arginine residues of the substrate in solution. Remarkably, immobilizing trypsin allows for the separation and thus, MS study on the sequences of truncated peptides in real time, leading to a time-resolved, "movie" of trypsin proteolysis. This work demonstrates the use of MOMs and co-crystallization to enhance the selectivity, catalytic efficiency, and stability of trypsin, suggesting the possibility of tuning the catalytic performance of a general protease using MOMs.

Introduction

Proteases hydrolyze peptide bonds at specific residues/sequences to decompose proteins into short peptides and thus, are essential for cellular functions and (potential) drug targets.[1-5] In spite of the promising progress in both fundamental structure-function relationship of proteases and their applications in biochemistry and biomedicine,[6-17] two key challenges, (*i*) the intrinsic instability (self-degradation) and (*ii*) the difficulty in depicting the catalytic process in real time, still hinder the further understanding of proteolytic mechanism, selectivity, and efficiency, and thus, need to be overcome.

Self-degradation not only prevents long-term storage and reuse/recycling of the costly protease, but also challenges the reliable study of the kinetics/mechanism of hydrolysis of a polypeptide substrate (but not the protease itself). Genetic modification may reduce the self-degradation,[18-20] yet this strategy may not be generalizable to all proteases while identifying the proper mutation(s) without hindering the native function requires special expertise. Pre-occupying the active site of a protease with a substitution of the substrate may reveal the proteolytic mechanism but prevent reusability or kinetics study.[16] Attaching proteases to solid supports may reduce self-degradation and allow for isolating the proteolytic products for mechanism study, yet chemical alteration to the protease or leaching would occur depending on the attaching methods.[21-23] In addition, large surface is not ideal for substrate contact while nanoscale surfaces face reduced protection against proteases on adjacent particles.[24-25] Thus, how to retain the stability of proteases during investigation remains challenging. The second challenge lies in the difficulty in accurately determining the sequences of the highly heterogeneous proteolytic products in real time yet this information is needed to reveal proteolytic selectivity and kinetics. Mass spectrometry (MS) is challenged by the need of rapid mass (peptide sequence) detection in real time (as protease

continues cleaving the substrate during MS detection),[26-28] so are other molecular size measurement techniques.[12, 20] It may be possible to quench the proteolytic reaction of certain proteases, yet this approach may not be generalizable to all proteases (without causing major disruptions of the target systems).

Here, we combine MOMs, SDSL-EPR, and MS to overcome both challenges. Metal-Organic Framework (MOFs) are advanced platforms to immobilize enzymes.[29-41] We recently found a unique approach to immobilize enzymes with large substrates (the size of a protein or larger) on porous solid supports based on the co-crystallization of enzyme and certain metals/ligands in the enzyme-friendly, aqueous phase (forming the enzyme@MOMs composites).[42-43] A portion of the enzymes can be exposed above the MOM crystal surface to contact large substrates, which cannot diffuse into MOM pores (~nm or smaller).[44-49] The buried portion allows for substantial protection against harsh environments including proteolytic conditions.[50] SDSL-EPR is sensitive to molecular rotational tumbling rates and thus, molecular size, as well as the population of the labeled peptides, regardless of the complexity of the studied system (protease and most MOMs do not influence EPR signal).[51-55] Thus, the molecular size and population of product polypeptides (if spin labeled on the truncation) can be monitored in real time by SDSL-EPR. Furthermore, immobilizing protease on MOFs/MOMs can ease the separation of the composites from the liquid phase in a reaction mixture, making it possible to study/identify the mass and sequences of the proteolytic products using tandem MS in real time. Comparing/combining EPR and MS results would thus, lead to a thorough and dynamic picture of the proteolytic reaction process.

To prove this strategy, we employ trypsin, a classic serine protease which cleaves peptides on the C-terminal end of lysine (K) and/or arginine (R), to degrade a model protein, T4 phage

lysozyme (T4L) in the solution state and upon immobilization on a Ca-MOM. The enzymatic kinetics were probed in real time by SDSL-EPR to monitor the population of the products of various T4L segments (selectively labeled by SDSL) upon proteolytic damage. We found significantly (at least 5-10 times) enhanced enzymatic efficiency for trypsin@Ca-MOMs as compared to free trypsin, an advantage of immobilizing proteases.[56-59] Surprisingly, trypsin@Ca-MOMs showed a preference in T4L regions to be cleaved, as compared to the non-selective cleavage of the whole protein in solution. Remarkably, being able to separate the cleaved T4L truncations from trypsin@Ca-MOM composites allowed us to use tandem MS to monitor the sequences of the broken T4L pieces over time, which were reasonably consistent with the EPR results but offered information of the ensemble of the product mixture with highly heterogeneous peptide length, sequence, and population. Lastly, we found excellent reusability of trypsin@Ca-MOMs as compared to trypsin in solution. This work represents the first study of co-crystallization of protease on Ca-MOMs, demonstrates the effectiveness of Ca-MOMs on enhancing protease selectivity, efficiency, and reusability, and suggests the possibility of using MOFs/MOMs to tune protease functionality/selectivity.

Results and Discussion

Preparation of the trypsin@Ca-MOM composite. The procedure to prepare trypsin@Ca-MOM composites in the aqueous phase follows our recent reports.[42] In brief, an aliquot of fresh commercial trypsin was solubilized in water with a final concentration of 0.017 mM. 50 μL of Ca^{2+} (0.5 M) and BPDC (0.25 M; converted to BPDC-Na_2 to enhance the solubility before the co-crystallization; details reported in the Supporting Information, SI) were then mixed with 1 mL of trypsin in water, followed by incubation at room temperature (RT) overnight under gentle shaking (40 rpm). The obtained co-crystals of trypsin@Ca-MOM were separated from the reaction mixture

via centrifugation, followed by wash with water for at least three times to remove the unreacted species. The supernatant of each wash was monitored until no protein was observed. The obtained co-crystals were stored in water at 4 ℃ for further use.

Basic characterization of the trypsin@Ca-BPDC composites. Scanning electron microscope (SEM) showed round/oval composites with roughly C-2 symmetry at a few μm length (Figure 1a), consistent with our Ca-BPDC work when encapsulating other enzymes.[42] The morphology was also confirmed by confocal fluorescence images (Figure 1b), wherein trypsin was covalently linked by fluorescein isothiocyanate (FITC) with unreacted species removed before co-crystallization with Ca^{2+} and BPDC in water (see the SI). The strong green fluorescence in Figure 1b indicates the successful encapsulation of trypsin, while the shape confirmed the morphology of the formed composites determined by SEM. To probe the crystallinity of the trypsin@Ca-BPDC composites, powder X-ray diffraction (PXRD) patterns were acquired for both Ca-BPDC and trypsin@Ca-BPDC composites. As shown in Figure 1c, the PXRD of trypsin@Ca-BPDC is almost superimposable with that of Ca-BPDC, the latter of which was simulated using a published Ca-BPDC structure.[42] Therefore, encapsulation of trypsin did not alter the crystallinity of Ca-BPDC significantly. Lastly, thermal gravimetric analysis (TGA) was carried out to further confirm the encapsulation of trypsin and estimate the loading capacity. As shown in Figure 1d, 1-2 % loading capacity was determined (w/w%), also consistent with the general loading capacity of Ca-BPDC as an enzyme immobilization platform.[42, 50] In particular, the decrease below 175 ℃ is originated by the decomposition of water while that between 240 and 500 ℃ is due to the decomposition of trypsin (see the righthand side of the y-axis and the weight loss at ~0.5 to 1.5% in the purple dots of Figure 1d). Taken together, our basic characterizations confirmed the success in the preparation of trypsin@Ca-BPDC composites. A schematic illustration of the structure of trypsin@Ca-BPDC

is shown in Figure 2a, along with the advantages of immobilizing trypsin protease on MOMs (Figure 2b).

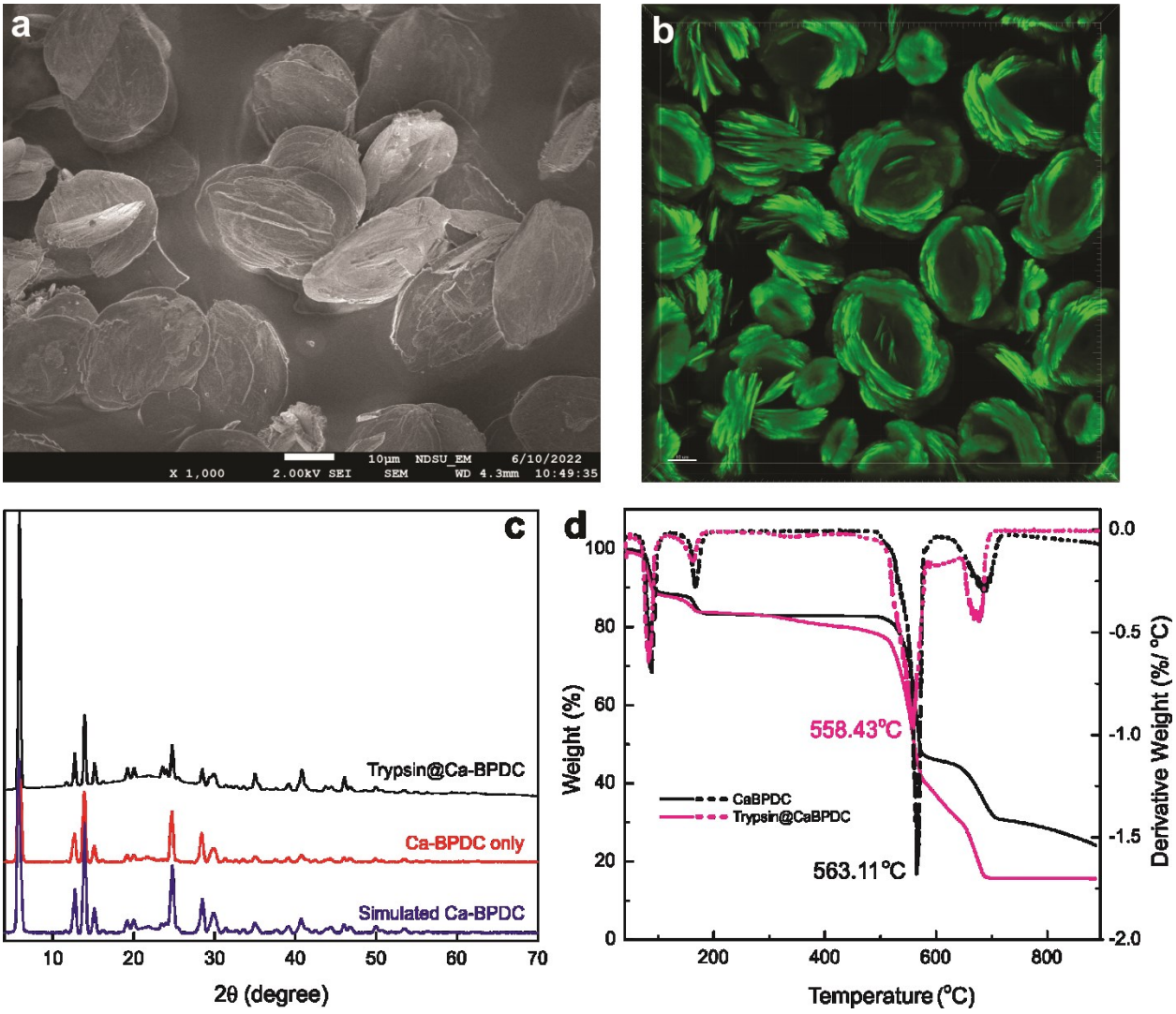

Figure 1. Basic characterization of the trypsin@Ca-BPDC composites. (a) SEM image of the prepared trypsin@Ca-BPDC. (b) Confocal fluorescence image of the FITC labeled trypsin@Ca-BPDC with an emission at 488 nm confirmed the presence of trypsin and the shape of the composites. The scale bar is 10 µm. (c) PXRD patterns of trypsin@Ca-BPDC (black), Ca-BPDC alone (red), and simulated pattern using published Ca-BPDC structures (blue). (d) TGA data of Ca-BPDC alone and trypsin@Ca-BPDC. The solid curves represent the Weight% while the

dotted curves represent the Derivative Weight % of Ca-BPDC alone (black) and trypsin@Ca-BPDC (purple).

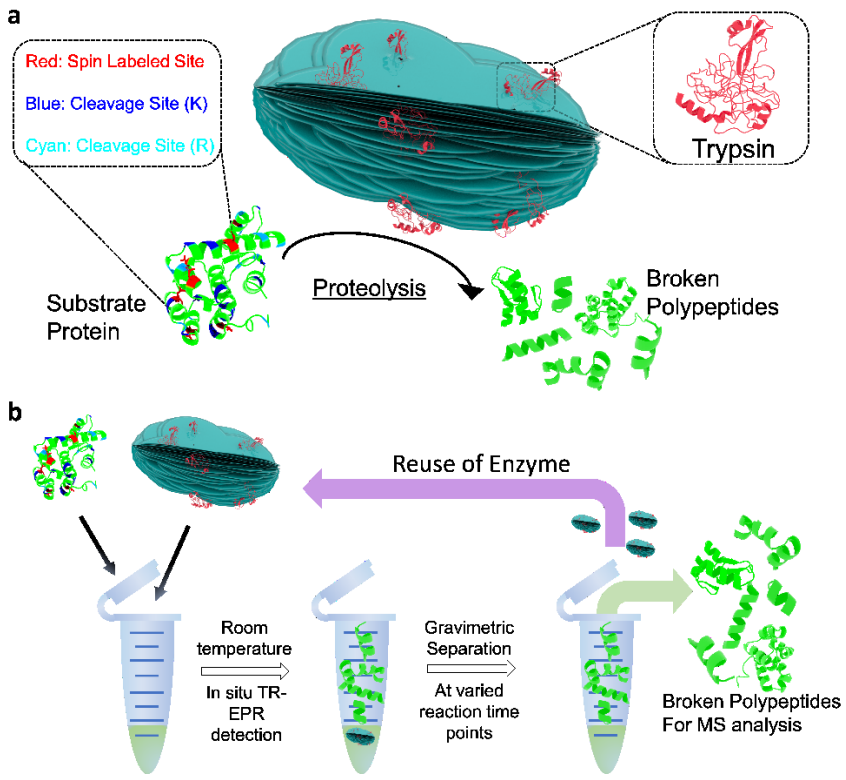

Figure 2. (A) Schematic illustration of the structure of trypsin@Ca-BPDC and its hydrolysis of a substrate protein. Trypsin is highlighted in red while T4L in green. The spin labeled sites, lysines, and arginines of T4L are highlighted in red, blue, and cyan on top of the T4L backbone, respectively. (B) Schematic illustration of the advantages of encapsulating trypsin on Ca-MOMs: enhanced reusability and the possibility of isolating products for molecular size and peptide sequence studies.

Analysis methods selection and principles. To confirm trypsin functionality, we employed the common approach to quantify protease activities based on a short polypeptide with optical or

fluorescent properties so that the breakdown of the peptide chain can cause a change in the spectrum. We have observed the expected catalytic performance and thus, demonstrated the activity of the selected commercial trypsin (Figure S1).

While this approach is commercially available, the practical operation can be complex (due to the various steps needed to generate the "coloring" effect) with relatively high uncertainties (due to the sensitivity of the optical/fluorescent method). More importantly, this approach is limited to proteins with optical or fluorescent changes upon cleavage. Fluorescent labeling of protein residues and probing the change in fluorescent quenching of protein tryptophan is an alternative, yet it can be limited by the location of native tryptophan and chemical perturbation of the substrate due to fluorescent labeling. Another alternative is to directly measure the structures of the cleaved substrate (polypeptide or protein) truncations using NMR. However, the heterogeneous and highly dynamic system (a mixture of cleaved and full-length proteins together with the protease) can complicate NMR spectral assignment and analysis. Tandem MS (MS/MS or MS^2) can reveal peptide segment sequences of the whole ensemble of the cleaved truncations yet it is difficult to carry out in real time because of the continuous degradation of the substrate (and thus, constant change in product composition) during MS/MS data acquisition. Here, we chose time-resolved SDSL-EPR to monitor representative segments/residues of a model protein substrate, which will not only identify the possible truncations of the broken protein segments (based on the cleavage residues and the spin labeled position) but also offer the relative preference of different protein regions being cleaved, if any. SDSL-EPR is a rapid measurement sensitive only to the labeled peptides regardless of the surround species in the ensemble in real time and does not rely on the presence of other residues (as compared to quenching measurements). The EPR results can be combined/compared with MS/MS if the products at each reaction time point can be separated from

the protease and subjected to MS study, which together will depict a dynamic picture of the whole proteolytic process.

The EPR principle to monitor protease activity is based on the sensitivity of EPR line shape to the molecular tumbling rate of a labeled peptide; the shorter the peptide, the faster the rate, and thus, the sharper the spectrum. Upon contact with the protease, the protein size begins to be reduced. The EPR spectrum usually contains one relatively broad component originated from the unreacted proteins and at least one sharp component as the labeled region is cleaved off from the main protein; the population of the broad component decreases over time while that of the sharp one increases as cleavage continues. The sharp component can become sharper over time if the labeled region is further cleaved into even smaller pieces. By monitoring the relative population of the sharp component for various protein regions, one can determine the proteolytic kinetics and reveal possible cleavage site selectivity. Note that as the proteolytic reaction continues, the peptide pieces can become so small that EPR loses sensitivity to their tumbling rates. Thus, through this work, we focused on only the first 30-40 min of EPR measurements; MS data were collected for a longer time due to the reduced enzyme activity in water, a required solvent for MS studies (see below).

Following these principles, we started by monitoring the 151R1 of T4L (see Figure 3; R1 represented the mutation of 151 residue to a cysteine and reacted with a spin probe as shown in the inset of Figure 3) upon contact with trypsin at a 0.175 mg/mL (7.35 μM) final concentration (with a fixed 0.05 mM T4L concentration) using time-resolved EPR. The resultant 2D EPR data are presented in Figure 4a, wherein for each peak (3 peaks are due to nitroxide hyperfine splitting), the sharp component reached to a plateau in ~ 2 h. Thus, this concentration and timeframe were selected through this work. This plot offers an opportunity to 1) obtain enzymatic kinetics if the

substrate concentration is varied, and 2) proteolytic site selectivity, if any, once different protein surface sites are studied, both of which are explored in this work.

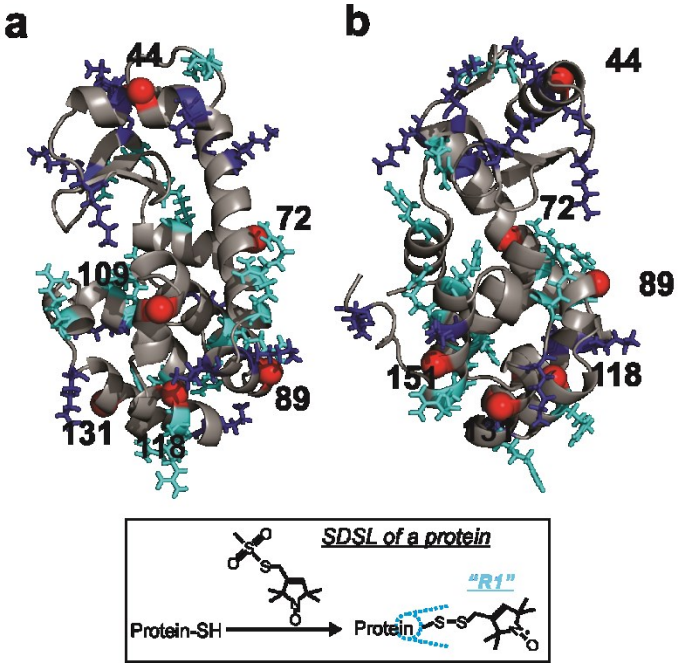

Figure 3. Locations of the spin labeled sites (red with residue number), lysines (blue), and arginines (cyan) on T4L protein substrate at two views differing by 180° (a and b). (inset) Illustration of SDSL of a protein cysteine residue (often generated by site-directed mutagenesis) with a spin label sidechain often designated by R1 for this particular nitroxide.

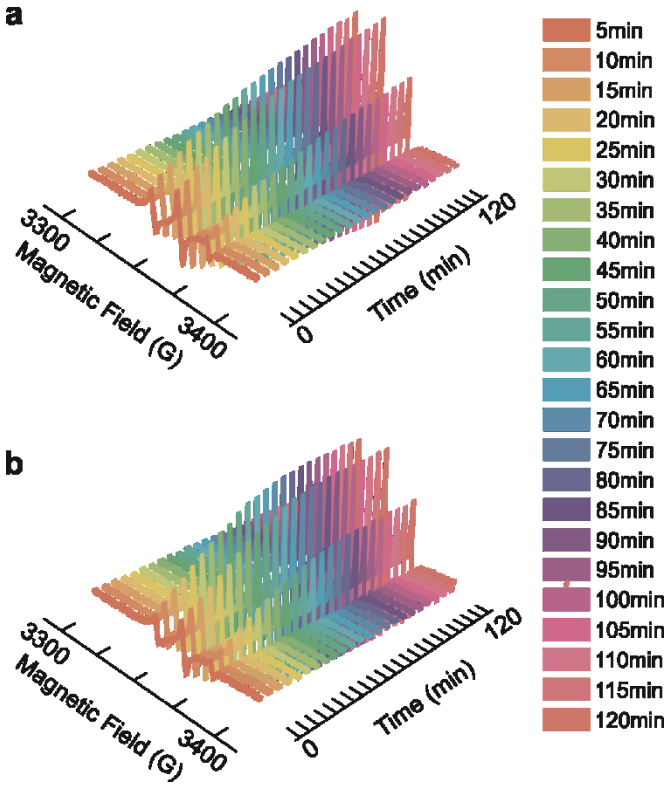

Figure 4. 2D-EPR data under the optimal trypsin concentration within 2 h time frame to degrade 151R1 of T4L using trypsin (a) and trypsin@Ca-BPDC (b).

Trypsin@Ca-BPDC enhanced trypsin catalytic efficiency. To probe the enzymatic kinetics, we employed the same trypsin concentration in solution and varied 151R1 concentrations. The EPR signal of each spectrum under different 151R1 concentrations and time points was plotted as a function of time (Figure S2a). The first 8 data points (0 to 40 min of reaction) was fit to a linear curve to obtain the relative reaction velocity, V_0 (Figure S3), followed by a plot of V_0 as a function of 151R1 concentration. A non-linear fitting based on the Michalis-Menten equation resulted in a k_m and V_{max} of 6.42 +/-2.09 mg/ml and 429.08 +/- 86.95 (in arbitrary unit, a.u.) (Figure 5a). Next, the same study was carried for trypsin@Ca-BPDC. Upon optimizing the composite amount (to roughly complete the cleavage within 2 h using 151R1 of T4L), we obtained the similar plot for

each labeled site (Figure 4b). Upon varying 151R1 concentration, we obtained the k_m and V_{max} of 1.91 +/- 0.82 mg/ml and 242.07 +/- 40.76 (arbitrary unit), respectively (Figure 5b). The reduced k_m indicates an enhanced binding affinity of trypsin@CaBPDC toward 151R1 as compared to free trypsin. The V_{max} of trypsin@CaBPDC is lower than that of free trypsin in buffer. However, this does not mean trypsin@CaBPDC has a lower catalytic efficiency.

In fact, to compare the catalytic efficiencies of enzymes, one often utilizes k_{cat}/k_m wherein k_{cat} is the turnover number which is related to V_{max} by $V_{max} = k_{cat}[E_{total}]$. We strived our best to maintain a close $[E_{total}]$ for trypsin (under the same reaction volume ~3.5 µg free trypsin and ~3.2 µg trypsin on Ca-BPDC were applied). Also, for an enzyme encapsulated in Ca-BPDC/MOF, although the precise amount of exposed enzyme cannot be determined, a rough estimate of ~30-40 % can be made based on prior studies of comparable systems;[42, 46] only these exposed trypsin can contact T4L (Ca-BPDC does not allow T4L diffusing through due to the small gap and the 3 x 3 x 5 nm dimension of T4L). Thus, the minimum k_{cat} of trypsin@CaBPDC should be 242.07/(3.2µg x 40%) ~ 189.06 (a.u.), slightly higher than that of free trypsin (429.08/3.5µg) ~122.59 (a.u.). Thus, the k_{cat}/k_m, the indicator of relative catalytic efficiency of enzymes, is at least 5 times larger for trypsin@CaBPDC (98.98 a.u.) than that of free trypsin (19.10 a.u.; calculations see Table S1). Note that the 40% exposure of trypsin on Ca-BPDC surface may not all be catalytically active (facing the active site toward the reaction medium). Thus, the roughly 5 times enhancement in catalytic efficiency enhancement is a minimum estimate. The true enhancement can be a factor of 10 if 50% of the exposed trypsin molecules orient their active sites toward the reaction medium. The similar trend is true if a different T4L mutant was selected for the enzymatic kinetic study, although the precise numbers may differ slightly. Thus, we believe that roughly a 5-10 times catalytic efficiency enhancement is offered by entrapping trypsin in Ca-MOM.

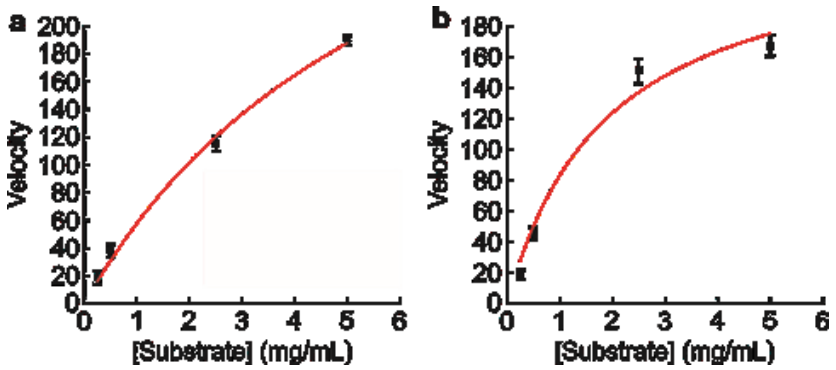

Figure 5. Determination of enzymatic kinetics when 151R1 was degraded by free trypsin (a) and trypsin@Ca-BPDC (b) using the Michaelis-Menten method. Uncertainty of each data point was obtained based on 3 repeats of the measurement of the reaction velocity.

Trypsin@Ca-BPDC enhanced catalytic selectivity. We started the selectivity study again with free trypsin in solution. A total of seven T4L sites (Figure 3) were labeled to scan across T4L molecule (containing 13 lysine and 13 arginine residues as potential cleavage sites). 2D EPR spectra of each labeled site are shown in Figures 4b and S6-S12 (representative 1-D EPR data shown in Figure S24). The spectrum of each mutant at each time point was then simulated using established methods which determine the best fitting parameters such as the rate and order of the motion of each component (broad and sharp component due to unfolded and folded protein portion) as well as the relative populations. Simulation details and best fit parameters are reported in the SI (Tables S2-S15; representative simulations shown in Figure S25). The plot of the sharp component's population as a function of time for each mutant is presented in Figure 6a (left) for the first 40 min. All labeled sites seemed to show a similar slope of increase for the sharp component, suggesting that all 7 sites were almost non-selectively hydrolyzed by trypsin. This is not a surprise given the high solvent-accessibility of most K and R residues of T4L (Figure 6a, right), the high tumbling and collision rates between the two proteins in solution, and the high

number of cleavage sites (13 K and 13 R residues) in the 164-residue T4L. As explained before, we cannot depict the sequences of peptide truncations during the catalysis due to the lack of time-resolved MS data.

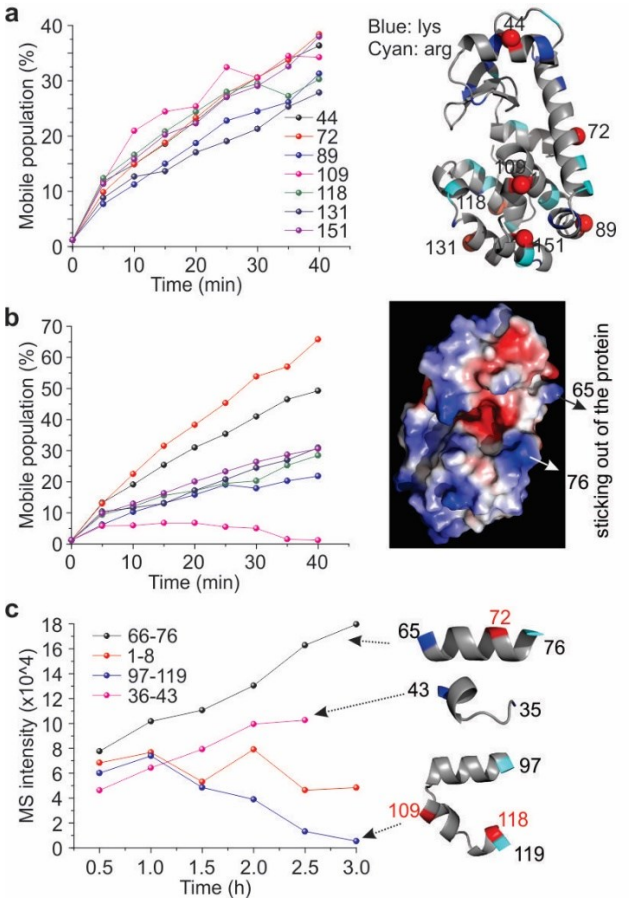

Figure 6. Monitoring the cleavage of different substrate protein regions. The population of the mobile phase (sharp spectral component) is plotted as a function of time for the first 40 min for different labelled sites of T4L upon hydrolysis by free trypsin (a) and trypsin@Ca-BPDC (b). The uncertainties in the populations of the mobile components are ~3% in our simulations. The distribution of the K and R residues (a) and the surface charge distribution for a T4L (b) may explain the proteolytic selectivity. (c) The highly populated peptide sequences obtained from time-resolved MS when T4L was cleaved by trypsin@Ca-BPDC (blue=K; cyan=R residues; red=spin labelled residues).

For trypsin@Ca-BPDC, we carried out the same 2D EPR studies (data see Figures S13-S19). Different from free trypsin, in the first 40 min, the population increase in the mobile/sharp component over time (Figure 6b, left) shows clear differences among different T4L mutants upon hydrolysis. Here, the mobile component of the spectra of 72R1 displays the highest rate of increase for the beginning 40 min of the cleavage, indicating at least one nearby K or R residues was preferentially selected by trypsin@Ca-BPDC. The second highest increase rate occurred at 44R1, followed by 89R1, 118R1, 131R1, and 151R1, the latter four of which showed a similar rate of increase. In contrast, the mobile component of 109R1 only increased in the first 5 min (flatting out and even dropping latter).

The rationalization of the site selectivity of trypsin@Ca-BPDC is as follows. Trypsin cleaves proteins at the positive K and R residues; for this to occur, a protein-trypsin contact is needed. Thus, exposed K and R residues with positive local surface charges may be preferred to be cleaved. At the early stage (<20 min), residue 72 is located at the external surface of the protein with two positive residues nearby, 65K and 76R, sticking out of the long helix of T4L (Figure 6b, right and S20), offering a higher chance for trypsin@Ca-BPDC to contact, possibly resulting in a truncation from 66 to 76. The cleavage of 43(K, also located at the outside surface) is close to 44R1, not only reducing the size of the segment containing 44R1 but also resulting in a faster motion because this cleavage left 44R1 at one end of the broken piece. 89R1, 131R1, and 151R1 show a similar extent of exposure with relatively close surrounding charge distributions, and thus, were cleaved with a similar preference. The nearest K and/or R residues for 109R1 are separated by 23 residues, cleavage of which would result in the longest chain with 109 labeled. The relatively high percentage of hydrophobic residues in this chain may entwine, aggregate, and/or adsorb to

the MOF surface, all of which would impose restrictions on site 109's motion. Such a restriction in 109's motion will reduce the population of the mobile component and shift it to the immobile region of the spectrum. Note that 118R is also in this long peptide. However, because the cleavage site is close to 118 (i.e. 119 is an arginine), even some restriction in motion would not reduce the mobility of 118 too much as 118 would be located at the end of the peptide with a high freedom in comparison to 109.

Time-resolved MS confirms EPR findings. The ease of separation of the trypsin@Ca-BPDC composite from all soluble species in the solution allows for the characterization of the ensemble of the substrate protein and hydrolyzed peptides. The raw data of MS shown in Figure S21 show a drop in the intensity of the peak originating from the protein (highlighted by the red block), confirming the reduction in molecular mass of T4L and thus, the cleavage of the protein substrate. Upon analysis of the MS/MS data, we found four peptide pieces with relatively high intensities through all studied time points (together with many other low-population peptide segments). We then plotted the population intensity of these four pieces as a function of time (Figure 6c, left). The segment of 66-76 shows a clear and strong increase in population, indicating that over time this segment is constantly generated upon interaction with trypsin@Ca-BPDC. Remarkably, 72R1 is located right on this segment which also shows a high increase in population based on the EPR data (Figures 6b and 6c, right). Segments 1-8 and 36-43 were both found in high populations over time (Figure 6c, right), indicating the N-terminus of the protein was cleaved preferentially, likely due to the relatively high positive charge distribution in this region (Figure S20b). This trend can also explain why 44R1 EPR data show a high rate of increase in the population of the cleaved substrate segments. Segment 97-109 shows an increase at the beginning followed by a decrease in population intensity. This trend is close to that of the 109R1 EPR data. A possible rationalization

would be that the entangled or aggregated long, hydrophobic peptide was adsorbed to the MOF surface or aggregated to deposit onto MOF and not effectively separated from the reaction mixture for MS detection. It may also be possible that the aggregated peptide's molecular mass is too large to be identified using the MS/MS analysis software. Nevertheless, we found a reasonable consistency between EPR and MS data, although these two techniques are sensitive to different segments/broken pieces (EPR: labeled segments/truncations; MS: the entire ensemble). Note that the time scale of MS is different from EPR because MS study requires a minimal amount of salts/buffer (ideally water) in the reaction medium, wherein the reaction rate can be lower than EPR studies which were all carried out in buffer.

To validate our rationalization of the EPR and MS data, we select the 66-76 truncation as a representative segment, due to the rapid increase in truncation population shown in both EPR and MS data. To confirm the cleavage site of 65K, we mutated this site to a cysteine and labeled with our R1 spin label (to avoid cysteine-based protein dimerization and remove the positive charge of lysine). Then, the 65R1 of T4L mutant was subjected to time-resolved MS study and the representative data are shown in Figure S22. Comparing Figures S22 and 6c indicates that the 66-76 truncation disappeared in 65R1, due to the mutation of the lysine at 65 to a cysteine-connected nitroxide. The site at 76 was still cleaved, resulting in the 61-76 truncation, which was generated in a much lower rate, confirming our speculation that 65K sticking out of the protein favors T4L contact with trypsin@Ca-BPDC. The other three dominant truncations were observed with a similar trend for each, as the mutation does not affect these regions.

Stability enhancement and reusability. To assess the effectiveness of Ca-BPDC on trypsin stabilization, we placed free trypsin and trypsin@Ca-BPDC at room temperature in buffer and acquired the time-resolved EPR data on one of the mutants (151R1) once per day for 10 days. The

relative catalytic activity is defined as the maximum EPR peak intensity over time (2 h). As is evident from Figure 7a, free trypsin lost 80 % activity after one day and even more on day 3. In contrast, trypsin@Ca-BPDC showed over 80 % activity even after 10 days' storage. These data confirmed that Ca-BPDC is effective in reducing self-degradation of trypsin, and possibly all proteases. We also probed the reusability of trypsin@Ca-BPDC composites and found almost no loss over 10 continuous reaction cycles (acquired over 5 days). Similar trend was observed when other labeled T4L mutants were employed for the reusability and stability studies (data not shown). Thus, Ca-BPDC effectively improved the stability and reusability of trypsin.

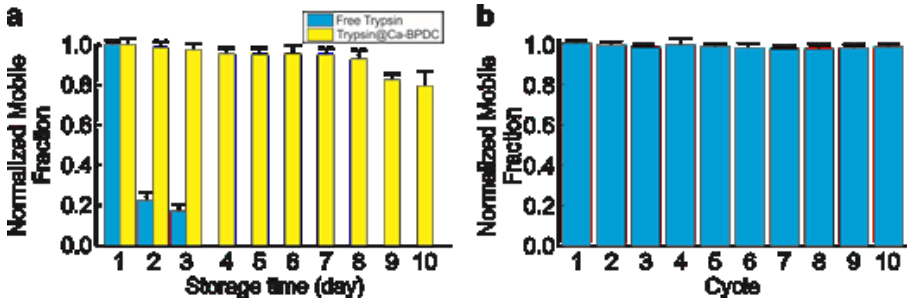

Figure 7. Stability and reusability of trypsin@Ca-BPDC. (a) The long-term storage stability of free trypsin (cyan) and trypsin@Ca-BPDC (yellow) as judged by the normalized intensity at the highest peak of EPR spectra. (b) The relative proteolytic activity of trypsin@Ca-BPDC upon 10 reuse cycles based on the normalized mobile peak intensity. Uncertainties were obtained from 3 repeats.

MOFs/MOMs allow for combining and comparing EPR and MS studies. Although MS/MS offers a direct detection of all truncated pieces of peptides in the entire ensemble, the practical challenge is to monitor the changes in the peptide in the ensemble over time (as protease will not stop cleaving the substrate upon contact in solution). EPR is sensitive to the motion of the broken

pieces (with a labeled site) over time yet cannot probe the whole ensemble. If combined, EPR and MS/MS in principle can reveal a thorough, dynamic picture of proteolytic kinetics and mechanism. MOFs/MOMs offer an opportunity to obtain time-resolved MS data, by gravimetrically separating the cleaved protein truncations from the insoluble protease@MOM composites and subjecting to sequence studies. This approach can be generalized to other proteases, keeping in mind that the synthetic condition of the protease@Ca-BPDC (or Ca-MOMs) is in the aqueous phase under ambient temperature/pressure, and thus, friendly to protease enzymes.

Influence of MOM platform on trypsin performance. A comprehensive comparison of our EPR results reveals the influence of MOMs on trypsin performance in terms of enzymatic efficiency and cleavage site preference. First, the k_{cat} / K_m values indicate at least 5 times enhancement (could easily be 10) in catalytic efficiency for trypsin upon encapsulation in Ca-BPDC (using our co-crystallization recipe). The absolute values of k_{cat} / K_m could not be accurately determined based on EPR intensity, yet a fair comparison can still be made when the same substrate and protease are employed as free enzyme or upon immobilization. For free trypsin in solution, the cleavage of a K or R residue of a substrate protein relies on the collision between the protein and trypsin as well as the chance for the K/R residue to collide with trypsin active site. Once immobilized on Ca-BPDC, some trypsin molecules always orient their active sites toward the reaction medium (some do not). Thus, as long as a protein collides the composite, the chance to be cleaved is high (given the high population of K/R residues in proteins). The layer-by-layer structure of the Ca-BPDC MOM and its ligand may also facilitate the adsorption of T4L onto it, further enhancing the effective contact of protein K/R residues with trypsin active sites. Lastly, during the reaction, without MOM, the free trypsin may degrade itself, also leading to reduced enzymatic efficiency.

Note that trypsin immobilized on other MOFs via different encapsulation approaches also showed enhanced proteolytic performance.[56, 60-61]

It has to be noted that our estimation of the catalytic efficiency enhancement was only based on a rough computation due to the difficulty in precisely determining the exposed protease amount and the percentage/probability of these proteases to place their active sites toward the reaction medium. At a complex interface such as the protease enzyme and Ca-MOMs, the only approach to determine this information is through SDSL and EPR spectroscopy, which can detect the probability of an enzyme residue to be exposed above the Ca-MOM crystal surface *versus* being buried under. However, it is difficult to carry out SDSL on protease enzymes due to the challenge of expressing the protease enzymes (as the protease may degrade itself during expression). Given the limited time and resources, in this work, we did not carry out a full SDSL-EPR study on trypsin. This will be explored as our future projects. Here we only employed a simplified, rough estimation of the catalytic efficiency based on prior studies of comparable systems when immobilizing enzymes on MOMs.[42,46] Our estimate could deviate substantially for trypsin or other protease enzymes. However, the general finding, immobilizing protease enhances proteolytic performance, is consistent with the literature.[56, 60-61]

Hosting trypsin in Ca-BPDC also leads to a preference of cleavage site against T4L protein. The solvent exposable 72R1 surrounded with positive local surface charges makes it a preferential site for Ca-BPDC and trypsin therein to contact and react with, as confirmed by both EPR and MS. The long peptide with a high tendency to entangle or aggregate did not affect the EPR line shape too much for free trypsin but may be adsorbed to the surface of Ca-BPDC. Thus, Ca-BPDC MOM not only enhances the enzymatic efficiency but also results in a cleavage site preference of trypsin protease. This is an important finding because Ca-MOMs essentially offers an effective approach

to tune the proteolytic/catalytic performance of protease enzymes, without chemically or genetically altering the protease! Such a finding is critical for protease engineering in many areas. A dynamic picture of the proteolytic reaction has been depicted based on the time-resolved EPR and MS results (Figure 8), where the four segments (i.e., 66-76) are cleaved with a higher preference and these truncations are present over time with increasing populations. The other cleavage sites were also cut yet with a lower preference.

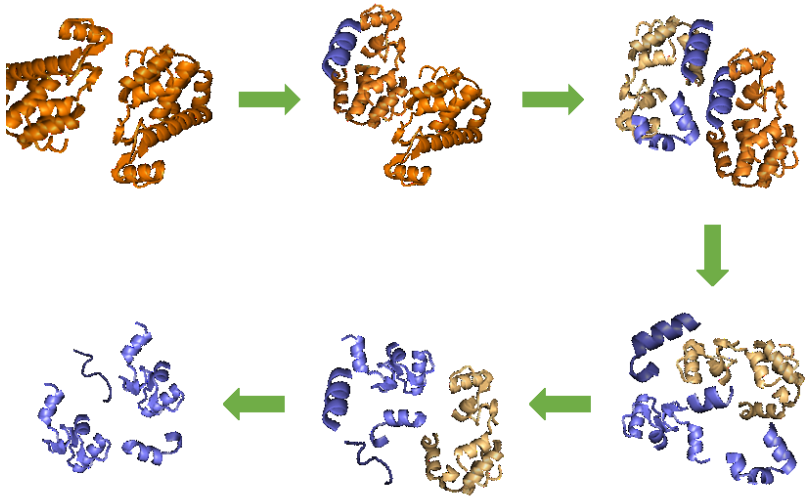

Figure 8. Schematic illustration of the cleavage process of T4L by trypsin@Ca-BPDC based on EPR and MS data.

MOFs/MOMs may potentially cause uncontrollable change in proteolytic selectivity and performance. The reality is that there are not enough data to come up with a generalizable conclusion of how MOFs/MOMs, or, the selection of metal ions and ligands, change protease performance, likely due to the difficulty in assessing protease substrate selectivity. Our work offered a practical approach to probe the regions of a globular protein (a protease' substrate) to be degraded, which can be generalized to other substrates. Our hope is to generate enough excitement so that SDSL-EPR in combination with MS can create a sufficient data base so that protease

immobilization on MOFs/MOMs can be custom made to optimize the proteolytic performance and substrate selectivity.

Conclusion

The overarching goal of this work is to overcome the two key challenges of protease research, (*i*) the intrinsic self-degradation and (*ii*) the difficulty in resolving the dynamic process of proteolysis in real time. To do so, we employed a recently developed MOM, Ca-BPDC, as the platform to immobilize a model protease, trypsin, on the crystal defects of the MOM via co-crystallization. This immobilization approach allows for partial exposure of trypsin on the Ca-BPDC surface and thus, direct contact with a model protein substrate, T4L. The hydrolysis of T4L by trypsin@Ca-BPDC was determined by a combination of SDSL-EPR and tandem MS techniques in real reaction time, wherein the former revealed enzymatic kinetics and possible cleavage site preference while the latter depicted the peptide sequences in the soluble mixture of the reaction ensemble. The results were compared to those without enzyme immobilization (trypsin in solution). We first found enhanced enzymatic efficiency (by a factor of 5-10) of trypsin once immobilized on Ca-BPDC in comparison to in solution. Surprisingly, EPR and MS results show that entrapping trypsin in our Ca-MOMs leads to a preference/selectivity in the cleavage site/region (in comparison to the non-selective cleavage of all K and R residues of the substrate in solution). This is the most intriguing finding of this work because it suggests the high potential of using MOFs/MOMs to tune protease functionality, critical for protease engineering. Remarkably, we were able to determine the sequences of cleaved peptides in the reaction mixture in real time, depicting the time-resolved process of trypsin proteolysis. This work demonstrates the use of MOMs and co-crystallization to enhance the selectivity, catalytic efficiency, and stability of

trypsin, and can possibly be generalized to general protease storage/recycling and kinetics/mechanism study.

Acknowledgements

This work is supported by the National Science Foundation (NSF: MCB 1942596) and National Institute of Food and Agriculture, United States Department of Agriculture Grant 2021-67021-34002. We appreciate Dr. Peter G. Fajer for generously donating the Bruker ECS-106 to our institution (North Dakota State University) and Dr. Wayne Hubbell for generously providing the EPR data analysis software.

Supporting Information

The Supporting Information is available free of charge at xxx.

Resources of chemical supplies, details of enzyme@MOF composite synthesis, basic characterization of the prepared composites, supporting characterization data, raw data of enzyme activity assay, and controls, and supporting tables of experimental observations and simulation parameters.

Competing Interests.

The authors declare no competing interests.

References

1. Powers, E. T.; Morimoto, R. I.; Dillin, A.; Kelly, J. W.; Balch, W. E., Biological and Chemical Approaches to Diseases of Proteostasis Deficiency. *Ann. Rev. Biochem.* **2009,** *78* (1), 959-991.
2. Neurath, H.; Walsh, K. A., Role of Proteolytic Enzymes in Biological Regulation (A Review). *Proc. Natl. Acad. Sci.* **1976,** *73* (11), 3825-3832.

3. Turk, B., Targeting Proteases: Successes, Failures and Future Prospects. *Nat. Rev. Drug Discov.* **2006,** *5* (9), 785-799.
4. Gurumallesh, P.; Alagu, K.; Ramakrishnan, B.; Muthusamy, S., A Systematic Reconsideration on Proteases. *Inter. J. Biol. Macromol.* **2019,** *128*, 254-267.
5. Drag, M.; Salvesen, G. S., Emerging Principles in Protease-Based Drug Discovery. *Nat. Rev. Drug Discov.***2010,** *9* (9), 690-701.
6. Vidmar, R.; Vizovišek, M.; Turk, D.; Turk, B.; Fonović, M., Protease Cleavage Site Fingerprinting by Label-Free In-Gel Degradomics Reveals ph-Dependent Specificity Switch of Legumain. *EMBO J.* **2017,** *36* (16), 2455-2465.
7. Hedstrom, L., Serine Protease Mechanism and Specificity. *Chem. Rev.* **2002,** *102* (12), 4501-4524.
8. Luthy, J. A.; Praissman, M.; Finkenstadt, W. R.; Laskowski, M., Detailed Mechanism of Interaction of Bovine β-Trypsin with Soybean Trypsin Inhibitor (Kunitz): I. STOPPED FLOW MEASUREMENTS. *J. Biol. Chem.* **1973,** *248* (5), 1760-1771.
9. Torbeev, V. Y.; Raghuraman, H.; Hamelberg, D.; Tonelli, M.; Westler, W. M.; Perozo, E.; Kent, S. B. H., Protein Conformational Dynamics in the Mechanism of HIV-1 Protease Catalysis. *Proc. Natl. Acad. Sci.* **2011,** *108* (52), 20982-20987.
10. Xue, Y.; Ha, Y., Catalytic Mechanism of Rhomboid Protease GlpG Probed by 3,4-Dichloroisocoumarin and Diisopropyl Fluorophosphonate. *J. Biol. Chem.* **2012,** *287* (5), 3099-3107.
11. Bagga, T.; Tulsian, N. K.; Mok, Y. K.; Kini, R. M.; Sivaraman, J., Mapping of Molecular Interactions between Human E3 Ligase TRIM69 and Dengue virus NS3 Protease using Hydrogen–Deuterium Exchange Mass Spectrometry. *Cell. Mol. Life Sci.* **2022,** *79* (5), 233.
12. Shao, F.; Vacratsis, P. O.; Bao, Z.; Bowers, K. E.; Fierke, C. A.; Dixon, J. E., Biochemical Characterization of the Yersinia YopT Protease: Cleavage Site and Recognition Elements in Rho GTPases. *Proc. Natl. Acad. Sci.* **2003,** *100* (3), 904-909.
13. Turk, B. E.; Huang, L. L.; Piro, E. T.; Cantley, L. C., Determination of Protease Cleavage Site Motifs using Mixture-Based Oriented Peptide Libraries. *Nat. Biotechnol.* **2001,** *19* (7), 661-667.
14. Saha, A.; Oanca, G.; Mondal, D.; Warshel, A., Exploring the Proteolysis Mechanism of the Proteasomes. *J. Phys. Chem. B* **2020,** *124* (27), 5626-5635.
15. Li, F.; Wang, Y.; Li, C.; Marquez-Lago, T. T.; Leier, A.; Rawlings, N. D.; Haffari, G.; Revote, J.; Akutsu, T.; Chou, K.-C.; Purcell, A. W.; Pike, R. N.; Webb, G. I.; Ian Smith, A.; Lithgow, T.; Daly, R. J.; Whisstock, J. C.; Song, J., Twenty Years of Bioinformatics Research for Protease-Specific Substrate and Cleavage Site Prediction: A Comprehensive Revisit and Benchmarking of Existing Methods. *Briefings Bioinformatics* **2019,** *20* (6), 2150-2166.
16. Radisky, E. S.; Lee, J. M.; Lu, C.-J. K.; Koshland, D. E., Insights into the Serine Protease Mechanism from Atomic Resolution Structures of Trypsin Reaction Intermediates. *Proc. Natl. Acad. Sci.* **2006,** *103* (18), 6835-6840.
17. Ramos-Guzmán, C. A.; Ruiz-Pernía, J. J.; Tuñón, I., Unraveling the SARS-CoV-2 Main Protease Mechanism Using Multiscale Methods. *ACS Catal.* **2020,** *10* (21), 12544-12554.
18. Baghban, R.; Farajnia, S.; Ghasemi, Y.; Mortazavi, M.; Ghasemali, S.; Zakariazadeh, M.; Zarghami, N.; Samadi, N., Engineering of Ocriplasmin Variants by Bioinformatics Methods for the Reduction of Proteolytic and Autolytic Activities. *Iran. J. Med. Sci.* **2021,** *46* (6), 454-467.

19. Liang, X.; Bian, Y.; Tang, X.-F.; Xiao, G.; Tang, B., Enhancement of Keratinolytic Activity of A Thermophilic Subtilase by Improving its Autolysis Resistance and Thermostability under Reducing Conditions. *Appl. Microbiol. Biotechnol.* **2010,** *87*, 999-1006.
20. Ye, Q.; Campbell, R. L.; Davies, P. L., Structures of Human Calpain-3 Protease Core with and without Bound Inhibitor Reveal Mechanisms of Calpain Activation. *J. Biol. Chem.* **2018,** *293* (11), 4056-4070.
21. Singh, A. N.; Singh, S.; Suthar, N.; Dubey, V. K., Glutaraldehyde-Activated Chitosan Matrix for Immobilization of A Novel Cysteine Protease, Procerain B. *J. Agricul. Food Chem.* **2011,** *59 11*, 6256-62.
22. Li, D.; Teoh, W. Y.; Gooding, J. J.; Selomulya, C.; Amal, R., Functionalization Strategies for Protease Immobilization on Magnetic Nanoparticles. *Adv. Funct. Mater.* **2010,** *20* (11), 1767-1777.
23. Diyanat, S.; Homaei, A.; Mosaddegh, E., Immobilization of Penaeus Vannamei Protease on ZnO Nanoparticles for Long-Term Use. *Inter. J. Biol. Macromol.* **2018,** *118*, 92-98.
24. Thakrar, F. J.; Singh, S. P., Catalytic, Thermodynamic and Structural Properties of An Immobilized and Highly Thermostable Alkaline Protease from A Haloalkaliphilic Actinobacteria, Nocardiopsis Alba TATA-5. *Bioresource Technol.* **2019,** *278*, 150-158.
25. Murugappan, G.; Sreeram, K. J., Nano-biocatalyst: Bi-functionalization of Protease and Amylase on Copper Oxide Nanoparticles. *Colloids Surfaces B Biointerfaces* **2021,** *197*, 111386.
26. Dodt, K.; Driessen, M. D.; Lamer, S.; Schlosser, A.; Lühmann, T.; Meinel, L., A Complete and Versatile Protocol: Decoration of Cell-Derived Matrices with Mass-Encoded Peptides for Multiplexed Protease Activity Detection. *ACS Biomater. Sci. Engineer.* **2020,** *6 12*, 6598-6617.
27. van den Berg, B. H. J.; Tholey, A., Mass Spectrometry-Based Proteomics Strategies for Protease Cleavage Site Identification. *Proteomics* **2012,** *12* (4-5), 516-529.
28. Schlüter, H.; Jankowski, J.; Rykl, J.; Thiemann, J.; Belgardt, S.; Zidek, W.; Wittmann, B.; Pohl, T., Detection of Protease Activities with the Mass-Spectrometry-Assisted Enzyme-Screening (MES) System. *Anal. Bioanal. Chem.* **2003,** *377*, 1102-1107.
29. Drout, R. J.; Robison, L.; Farha, O. K., Catalytic Applications of Enzymes Encapsulated in Metal-Organic Frameworks. *Coord. Chem. Rev.* **2019,** *381*, 151-160.
30. Li, P.; Chen, Q.; Wang, T. C.; Vermeulen, N. A.; Mehdi, B. L.; Dohnalkova, A.; Browning, N. D.; Shen, D.; Anderson, R.; Gómez-Gualdrón, D. A.; Cetin, F. M.; Jagiello, J.; Asiri, A. M.; Stoddart, J. F.; Farha, O. K., Hierarchically Engineered Mesoporous Metal-Organic Frameworks toward Cell-free Immobilized Enzyme Systems. *Chem* **2018,** *4* (5), 1022-1034.
31. Majewski, M. B.; Howarth, A. J.; Li, P.; Wasielewski, M. R.; Hupp, J. T.; Farha, O. K., Enzyme Encapsulation in Metal-Organic Frameworks for Applications in Catalysis. *CrystEngComm* **2017,** *19* (29), 4082-4091.
32. Wang, X.; Lan, P. C.; Ma, S., Metal-Organic Frameworks for Enzyme Immobilization: Beyond Host Matrix Materials. *ACS Centr. Sci.* **2020,** *6*, 1497-1506.
33. Gkaniatsou, E.; Sicard, C. m.; Ricoux, R. m.; Mahy, J.-P.; Steunou, N.; Serre, C., Metal-Organic Frameworks: A Novel Host Platform for Enzymatic Catalysis and Detection. *Mater. Horiz.* **2017,** *4* (1), 55-63.
34. Kirchon, A.; Feng, L.; Drake, H. F.; Joseph, E. A.; Zhou, H.-C., From Fundamentals to Applications: A Toolbox for Robust and Multifunctional MOF Materials. *Chem. Soc. Rev.* **2018,** *47* (23), 8611-8638.

35. Lian, X.; Fang, Y.; Joseph, E.; Wang, Q.; Li, J.; Banerjee, S.; Lollar, C.; Wang, X.; Zhou, H.-C., Enzyme-MOF (Metal-Organic Framework) Composites. *Chem. Soc. Rev.* **2017,** *46* (11), 3386-3401.
36. Liang, W.; Wied, P.; Carraro, F.; Sumby, C. J.; Nidetzky, B.; Tsung, C.-K.; Falcaro, P.; Doonan, C. J., Metal–Organic Framework-Based Enzyme Biocomposites. *Chem. Rev.* **2021,** *121* (3), 1077-1129.
37. Liang, W.; Xu, H.; Carraro, F.; Maddigan, N. K.; Li, Q.; Bell, S. G.; Huang, D. M.; Tarzia, A.; Solomon, M. B.; Amenitsch, H.; Vaccari, L.; Sumby, C. J.; Falcaro, P.; Doonan, C. J., Enhanced Activity of Enzymes Encapsulated in Hydrophilic Metal-Organic Frameworks. *J. Am. Chem. Soc.* **2019,** *141* (6), 2348-2355.
38. Liang, K.; Ricco, R.; Doherty, C. M.; Styles, M. J.; Bell, S.; Kirby, N.; Mudie, S.; Haylock, D.; Hill, A. J.; Doonan, C. J.; Falcaro, P., Biomimetic Mineralization of Metal-Organic Frameworks as Protective Coatings for Biomacromolecules. *Nat. Commun.* **2015,** *6*, 7240.
39. Wu, Y.; Chen, H.; Chen, Y.; Sun, N.; Deng, C., Metal Organic Frameworks as Advanced Extraction Adsorbents for Separation and Analysis in Proteomics and Environmental Research. *Sci. China Chem.* **2022,** *65* (4), 650-677.
40. Du, Y.; Jia, X.; Zhong, L.; Jiao, Y.; Zhang, Z.; Wang, Z.; Feng, Y.; Bilal, M.; Cui, J.; Jia, S., Metal-Organic Frameworks with Different Dimensionalities: An Ideal Host Platform for Enzyme@MOF Composites. *Coord. Chem. Rev.* **2022,** *454*, 214327.
41. Lu, J.; Wu, J.-K.; Jiang, Y.; Tan, P.; Zhang, L.; Lei, Y.; Liu, X.-Q.; Sun, L.-B., Fabrication of Microporous Metal–Organic Frameworks in Uninterrupted Mesoporous Tunnels: Hierarchical Structure for Efficient Trypsin Immobilization and Stabilization. *Angew. Chem. Int. Ed.* **2020,** *132* (16), 6490-6496.
42. Pan, Y.; Li, Q.; Li, H.; Farmakes, J.; Ugrinov, A.; Zhu, X.; Lai, Z.; Chen, B.; Yang, Z., A General Ca-MOM Platform with Enhanced Acid/Base Stability for Enzyme Biocatalysis. *Chem Catal.* **2021,** *1*, 146-161.
43. Pan, Y.; Li, H.; Lenertz, M.; Han, Y.; Ugrinov, A.; Kilin, D.; Chen, B.; Yang, Z., One-pot Synthesis of Enzyme@Metal-Organic Materials (MOM) Biocomposites for Enzyme Biocatalysis. *Green Chem.* **2021,** *33*, 4466-4476.
44. Pan, Y.; Li, H.; Li, Q.; Lenertz, M.; Schuster, I.; Jordahl, D.; Zhu, X.; Chen, B.; Yang, Z., Protocol for Resolving Enzyme Orientation and Dynamics in Advanced Porous Materials via SDSL-EPR. *STAR Protoc.* **2021,** *2* (3), 100676.
45. Pan, Y.; Li, H.; Li, Q.; Lenertz, M.; Zhu, X.; Chen, B.; Yang, Z., Site-Directed Spin Labeling-Electron Paramagnetic Resonance Spectroscopy in Biocatalysis: Enzyme Orientation and Dynamics in Nanoscale Confinement. *Chem Catal.* **2021,** *1*, 207-231.
46. Pan, Y.; Li, H.; Farmakes, J.; Xiao, F.; Chen, B.; Ma, S.; Yang, Z., How Do Enzymes Orient on Metal-Organic Framework (MOF) Surfaces? *J. Am. Chem. Soc.* **2018,** *140*, 16032-16036.
47. Li, Q.; Pan, Y.; Li, H.; Alhalhooly, L.; Li, Y.; Chen, B.; Choi, Y.; Yang, Z., Size-tunable Metal-Organic Framework Coated Magnetic Nanoparticles for Enzyme Encapsulation and Large-Substrate Biocatalysis. *ACS Appl. Mater. Interfaces* **2020,** *12*, 41794-41801.
48. Neupane, S.; Patnode, K.; Li, H.; Baryeh, K.; Liu, G.; Hu, J.; Chen, B.; Pan, Y.; Yang, Z., Enhancing Enzyme Immobilization on Carbon Nanotubes via Metal-Organic Frameworks for Large-Substrate Biocatalysis. *ACS Appl. Mater. Interfaces* **2019,** *11* (12), 12133-12141.
49. Farmakes, J.; Schuster, I.; Overby, A.; Alhalhooly, L.; Lenertz, M.; Li, Q.; Ugrinov, A.; Choi, Y.; Pan, Y.; Yang, Z., Enzyme Immobilization On Graphene Oxide (GO) Surface via One-

Pot Synthesis of GO/Metal-Organic Framework Composites for Large-Substrate Biocatalysis. *ACS Appl. Mater. Interfaces* **2020,** *12* (20), 23119-23126.
50. Li, Q.; Pan, Y.; Li, H.; Lenertz, M.; Reed, K.; Jordahl, D.; Bjerke, T.; Ugrinov, A.; Chen, B.; Yang, Z., Cascade/Parallel Biocatalysis via Multi-Enzyme Encapsulation on Metal-Organic Materials for Rapid and Sustainable Biomass Degradation. *ACS Appl. Mater. Interfaces* **2021,** *13*, 43085–43093.
51. Budil, D. E.; Lee, S.; Saxena, S.; Freed, J. H., Nonlinear-Least-Squares Analysis of Slow-Motion EPR Spectra in One and Two Dimensions Using a Modified Levenberg-Marquardt Algorithm. *J. Magn. Reson. A* **1996,** *120* (2), 155-189.
52. Hubbell, W. L.; Altenbach, C., Investigation of Structure and Dynamics in Membrane Proteins using Site-Directed Spin Labeling. *Curr. Opin. Struct. Biol.* **1994,** *4* (4), 566-573.
53. Hubbell, W. L.; Gross, A.; Langen, R.; Lietzow, M. A., Recent Advances in Site-Directed Spin Labeling of Proteins. *Curr. Opin. Struct. Biol.* **1998,** *8* (5), 649-656.
54. Hubbell, W. L.; López, C. J.; Altenbach, C.; Yang, Z., Technological Advances in Site-Directed Spin Labeling of Proteins. *Curr. Opin. Struct. Biol.* **2013,** *23* (5), 725-733.
55. Pan, Y.; Neupane, S.; Farmakes, J.; Oh, M.; Bentz, K.; Choi, Y.; Yang, Z., Insights on the Structure, Molecular Weight and Activity of an Antibacterial Protein-Polymer Hybrid. *ChemPhysChem* **2018,** *19* (5), 651-658.
56. Zhong, C.; Lei, Z.; Huang, H.; Zhang, M.; Cai, Z.; Lin, Z., One-pot Synthesis of Trypsin-based Magnetic Metal–Organic Frameworks for Highly Efficient Proteolysis. *J. Mater. Chem. B* **2020,** *8* (21), 4642-4647.
57. Yue, Q.; Li, J.; Luo, W.; Zhang, Y.; Elzatahry, A. A.; Wang, X.; Wang, C.; Li, W.; Cheng, X.; Alghamdi, A.; Abdullah, A. M.; Deng, Y.; Zhao, D., An Interface Coassembly in Biliquid Phase: Toward Core–Shell Magnetic Mesoporous Silica Microspheres with Tunable Pore Size. *J. Am. Chem. Soc.* **2015,** *137* (41), 13282-13289.
58. Kandambeth, S.; Venkatesh, V.; Shinde, D. B.; Kumari, S.; Halder, A.; Verma, S.; Banerjee, R., Self-templated Chemically Stable Hollow Spherical Covalent Organic Framework. *Nat. Commun.* **2015,** *6* (1), 6786.
59. Chao, H.; Zhou, Z.; He, W.; Li, M.; Yuan, X.; Su, P.; Song, J.; Yang, Y., Template-Free In Situ Encapsulation of Enzymes in Hollow Covalent Organic Framework Capsules for the Electrochemical Analysis of Biomarkers. *ACS Appl. Mater. Interfaces* **2022,** *14* (18), 20641-20651.
60. Navarro-Sánchez, J.; Almora-Barrios, N.; Lerma-Berlanga, B.; Ruiz-Pernía, J. J.; Lorenz-Fonfria, V. A.; Tuñón, I.; Martí-Gastaldo, C., Translocation of Enzymes into A Mesoporous MOF for Enhanced Catalytic Activity under Extreme Conditions. *Chem. Sci.* **2019,** *10* (14), 4082-4088.
61. Badoei-dalfard, A.; Khankari, S.; Karami, Z., One-pot Synthesis and Biochemical Characterization of Protease Metal Organic Framework (Protease@MOF) and its Application on the Hydrolysis of Fish Protein-Waste. *Colloids Surfaces B Biointerfaces* **2020,** *196*, 111318.


Trypsin
or
MOF